Ultrasonic Study of the Properties of the Ferrous and Ferric Ions in Corundum*

J. LEWINER
Laboratorie d'Electricité Générale, Ecole Supérieure de Physique et de Chimie, Paris, France
AND
PAUL H. E. MEIJER
Department of Physics, Catholic University, Washington, D. C. 20017
(Received 20 October 1969)

Acoustic paramagnetic resonance was observed directly for the first time in Fe^{3+}-doped Al_2O_3 at 9366 MHz using fields between 0 and 5000 G in various directions. The transitions were identified by comparing the angular dependence of the resonance lines with the theoretically expected positions. From the observed attenuation for each line in conjunction with the matrix elements of the interaction Hamiltonian, it was possible to determine some of the elements of the magnetoelastic coupling tensor. The following values were found: $[\frac{1}{4}(G_{11}-G_{12})^2+G_{16}^2]^{1/2}=0.42\pm0.11$ cm^{-1}/(unit strain); $[G_{52}^2+G_{41}^2]^{1/2}=2.9\pm0.9$ cm^{-1}/(unit strain) for Fe^{3+}. In order to obtain these values, we calculated explicitly the line shape as a function of the field strength. One line was identified as an Fe^{2+} line. The dependence of the attenuation of this line on the angle was in complete agreement with our predictions. A comparison is made with experimental data obtained for the magnetoelastic tensor using EPR experiments under stress, and with available theories.

I. INTRODUCTION

IT is well known that the spin-lattice relaxation of the iron group ions is due to the Kronig–Van Vleck mechanism,[1–3] based on the modulation of the crystalline field by the phonons.

For a long time the only experimental way to obtain information on the spin phonon interaction was to measure the spin lattice relaxation time in an electron-paramagnetic-resonance (EPR) experiment and to try to relate it to the coupling constants. In the last few years, two methods have been developed in order to measure these constants directly. One is the EPR experiment under uniaxial stress. In this method uniaxial stress or strain is applied to the paramagnetic crystal and the ions of the lattice are displaced from their equilibrium position. This creates a slight change in the electric crystalline field which in turn produces a shift of the energy levels of the spin system. The values of the resonant magnetic field are then shifted and these shifts are measured for different directions of the applied stress or strain, and they can be used to calculate the magnetoelastic coefficients of the ion. The other one is the method of acoustic paramagnetic resonance (APR). In APR experiment transitions between the lowest levels of an ion in its crystalline environment are excited by an ultrasonic wave. The resonance is detected by measuring the sound attenuation coefficient as a function of an applied magnetic field. From the intensity of the absorption line it is possible to calculate the magnetoelastic coefficients.

The difference between these two methods is that in the first the stress or strain is applied statically whereas in the second it is applied dynamically.

In this work we will describe the APR method which has been used to calculate the Fe^{3+} coupling constants in corundum. In this ion the spin-phonon interaction is expected to be small, since the orbital ground state is an S state and the first-order perturbation is zero. Second- and higher-order mechanisms must be used to calculate the interaction and this involves excited states of the ion.

In Sec. II, we give the theory based on the spin Hamiltonian formalism. In Sec. III, we present the experimental procedure. Sec. IV contains the experimental data and their analysis. The conclusion is given in Sec. V.

II. THEORY

A. Phenomenological Description of Spin-Phonon Interaction

It was shown by Pryce[4] and Abragam and Pryce[5] that the splitting of the ground state of an iron group ion can be described in terms of a spin Hamiltonian with an effective spin S. A general expression for this Hamiltonian is

$$\mathcal{H}=\beta H\cdot g\cdot S+S\cdot D\cdot S. \quad (1)$$

In this expression g and D are related to the static nondeformed lattice. Terms of order S^4 and higher which may be of importance in some cases have been omitted.

A phenomenological interaction Hamiltonian was proposed by Dobrov[6] based on the following arguments.

Let the spin Hamiltonian for a uniformly strained attice be

$$\mathcal{H}=\beta H\cdot g\cdot S+S\cdot D\cdot S+\beta H\cdot dg\cdot S+S\cdot d\cdot S,$$

* Part of this work was supported by the CNRS and NASA Grant No. NSG 647/07-05-008.

[1] R. de L. Kronig, Physica **6**, 33 (1936).
[2] J. H. Van Vleck, J. Chem. Phys. **1**, 72 (1939).
[3] J. H. Van Vleck, Phys. Rev. **57**, 426 (1940).
[4] M. H. L. Pryce, Proc. Phys. Soc. (London) **A63**, 25 (1950).
[5] A. Abragam and M. H. L. Pryce, Proc. Roy. Soc. (London) **A205**, 135 (1951).
[6] W. I. Dobrov, Phys. Rev. **134**, A734 (1964).

where dg and d are the deviations from the equilibrium values g and D. As they are functions of the strain, they can be considered as operators for the phonon field writing

$$\mathcal{H}_{\text{int}}=\beta H\cdot dg\cdot S+S\cdot d\cdot S. \quad (2)$$

The first term of $\mathcal{H}_{\text{int}}$ is called the dipolar term, the second one is called the quadrupolar term. The relation of dg and d to the strain of the lattice is given by

$$dg_{ij}=\sum_{kl} F_{ijkl}\epsilon_{kl} \quad \text{and} \quad d_{ij}=\sum_{kl} G_{ijkl}\epsilon_{kl}.$$

Here the constants F_{ijkl} and G_{ijkl} are the elements of fourth-order tensors F and G, the dipolar and quadrupolar magnetoelastic tensors, respectively, ϵ_{kl} is the klth component of the strain. The tensors F and G can be written with the Voigt notation,[7,8] as 6 by 6 matrices. The number of independent coefficients depends on the symmetry of the crystal. They have been tabulated for many symmetries by Fumi.[9,10]

It has been shown[11,12] that the quadrupolar term is in general much larger than the dipolar term. When the wave functions of the levels concerned are such that the matrix elements of the quadrupolar coupling are not zero, we will neglect the dipolar term. The quadrupolar term can be written as

$$\mathcal{H}_{\text{quad}}=d_{xx}S_x^2+d_{yy}S_y^2+d_{zz}S_z^2+d_{yz}(S_yS_z+S_zS_y)+d_{xz}(S_xS_z+S_zS_x)+d_{xy}(S_xS_y+S_yS_x).$$

Introducing the operators $S_+=S_x+iS_y$ and $S_-=S_x-iS_y$, we can write

$$\mathcal{H}_{\text{quad}}=\tfrac{1}{2}\{[\tfrac{1}{2}(d_{xx}-d_{yy})-id_{xy}]S_+^2+[\tfrac{1}{2}(d_{xx}-d_{yy})+id_{xy}]S_-^2\}+\tfrac{1}{2}[(d_{xz}-id_{yz})\times(S_+S_z+S_zS_+)+(d_{xz}+id_{yz})(S_-S_z+S_zS_-)]+[d_{zz}S_z^2+\tfrac{1}{2}(d_{xx}+d_{yy})(S^2-S_z^2)]. \quad (3)$$

The three terms of Eq. (3) consist of the matrix elements of $\mathcal{H}_{\text{quad}}$ with $\Delta m=\pm 2$, ± 1, and 0, respectively.

In the above we have not considered the effect of the phonons on the excited states of the ion which give rise to additional terms in $\mathcal{H}_{\text{int}}$.[12] We have found that they can be neglected in the present case.

B. Acoustic Paramagnetic Resonance

The amplitude of the induced strain in a paramagnetic crystal in presence of an ultrasonic wave is given by the relation

$$\epsilon(l,t)=\epsilon[e^{i(\omega t-kl)}]e^{-\alpha_t l}.$$

In this expression ω is the frequency of the ultrasonic wave, α_t the attenuation coefficient, and the wave vector k is related to the phase velocity v of the phonon mode by the relation

$$k=\omega/v.$$

The energy flux associated with the wave can be written as

$$E=E_0e^{-2\alpha_t l}.$$

The attenuation coefficient can then be defined by

$$\frac{\Delta E}{E}=2\alpha_t l\Delta l \quad \text{and} \quad \alpha_t=\alpha_0+\alpha.$$

ΔE is the energy lost by the sound wave in a volume of unit cross section and length Δl, E is the acoustic flux, α_0 is the normal part of the attenuation of the sound in the crystal, and α is the part due to the paramagnetic resonance.

Let U be the probability of transition between two levels of the spin system due to exchange of energy with the phonons. Since all the work which will be described here was done at liquid helium temperatures, we will neglect Raman and multiple quantum processes.

Let n be the number of spins per unit volume which absorb energy. Then $\Delta E=n\hbar\omega U\Delta l$. The acoustic flux is given by the relation $E=\frac{1}{2}\rho v^3\epsilon^2$ where ρ is the mass density of the crystal.

$$\frac{\Delta E}{E}=\frac{2n\hbar\omega U\Delta l}{\rho\epsilon^2v^3}=2\alpha\Delta l \quad \text{and} \quad \alpha=\frac{n\hbar\omega U}{\rho\epsilon^2v^3}. \quad (4)$$

U is obtained from the time dependent perturbation theory and is given by

$$U=\frac{1}{4\hbar^2}|\langle|\mathcal{H}_{\text{int}}|\rangle|^2g(\nu),$$

where $g(\nu)$ is the absorption line shape. Introducing this value of U in Eq. (4) we have

$$\alpha=\frac{n\omega|\langle|\mathcal{H}_{\text{int}}|\rangle|^2}{4\rho\epsilon^2v^3\hbar}g(\nu). \quad (5)$$

In general the experimental parameter is not the frequency of the ultrasonic wave but the magnetic field H. It is then necessary to calculate the absorption line shape as a function of the field $f(H)$, which can only be done when the energy-level system is known analytically. The energy difference and the frequency are connected by the universal relation $E_i-E_j=h\nu$. There is no such universal relation between the energy difference and the magnetic field. If $F(H)=h\nu$ one has

$$E_i-E_j=F(H).$$

[7] J. F. Nye, *Physical Properties of Crystals* (Oxford University Press, New York, 1957).
[8] R. R. Birss, *Symmetry and Magnetism* (North-Holland Publishing Co., Amsterdam, 1964).
[9] F. G. Fumi, Acta Cryst. 5, 44 (1952); 5, 691 (1952).
[10] F. G. Fumi, Nuovo Cimento 9, 739 (1952).
[11] R. D. Mattuck and M. W. P. Strandberg, Phys. Rev. Letters 3, 369 (1959).
[12] M. W. P. Strandberg and R. D. Mattuck, Phys. Rev. 119, 1284 (1960).

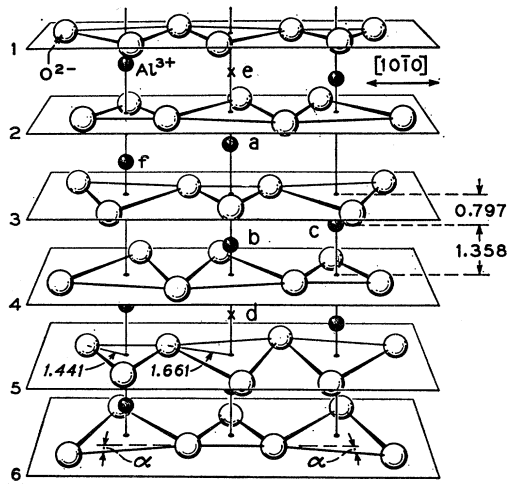

FIG. 1. The Al_2O_3 lattice. The c axis is perpendicular to the plane of the oxygens (the open circles). Through a 60° rotation around the c axis one goes from one equivalent aluminum site to the other.

Since $g(\nu)$ and $f(H)$ must be normalized, one has

$$\int g(\nu)d\nu=\int f(H)dH=1,$$

and therefore

$$f(H)=\frac{d\nu}{dH}g(\nu). \tag{6}$$

Two simple cases can be considered where the energy levels are linear with the magnetic field. The first one is the case of a $\Delta m=1$ transition.

$F(H)=g\beta H+$const and therefore $f(H)=g(\nu)g\beta/h$. The second one is the case of a $\Delta m=2$ transition. $F(H)=2g\beta H+$const, which leads to $f(H)=2g(\nu)g\beta/h$.

In the general case it is necessary to know the analytical expression of $F(H)$, if this is not possible then an approximation can be found by computer.

Relation (5) can be written as a function of $f(H)$

$$\alpha=\frac{n\omega|\langle|\mathcal{H}_{\rm int}|\rangle|^2\pi}{2\rho\epsilon^2v^3}\frac{dH}{d\nu}f(H).$$

We will assume in the following that the lines have a Lorentzian shape. In that case we have

$$f(H)=\frac{1/\pi\delta}{1+(H-H_0)^2/\delta^2}.$$

In this expression δ is the half-width of the line.

C. Properties of Fe^{3+} in Al_2O_3 and Ultrasonic Transitions

The Al_2O_3 lattice as described by Geschwind and Remeika[13] is shown in Fig. 1. It exhibits a threefold rotational symmetry around an axis perpendicular to the planes of the oxygen ions. Although the maximum-point group symmetry of the crystal lattice is $\bar{3}m$, each Al^{3+} or Fe^{3+} has only a three-point group symmetry. The different sites for the Al^{3+} ions are physically equivalent, however two magnetically nonequivalent sites can be observed. For instance in Fig. 1 sites b and c are equivalent. They are not equivalent to sites a and f. They can be derived from the latter by a 60° rotation around the trigonal axis.

The free ion Fe^{3+} has the $3d^5$ electronic configuration. The $3d$ electronic shell is half filled and the resultant orbital momentum is equal to zero. The singlet ground state ^6S has a sixfold spin degeneracy. When it is introduced in the Al_2O_3 lattice, Fe^{3+} takes the place of an Al^{3+} ion. The crystalline field has a trigonal symmetry component and a cubic part. The angular momentum $J=S=\frac{5}{2}$ is split into three Kramers doublets. The splitting of the lowest orbital level can be described in terms of a spin Hamiltonian[14]:

$$\begin{aligned}\mathcal{H}=&g\beta H\cdot S+D[S_z^2-\tfrac{1}{3}S(S+1)]\\&+(F/180)[35S_z^2-30S(S+1)S_z^2+25S_z^2\\&-6S(S+1)+3S^2(S+1)^2]\\&+(a/6)[S_\xi^4+S_\eta^4+S_\zeta^4-\tfrac{1}{5}S(S+1)(3S^2-3S-1)].\end{aligned}$$

In this expression ξ, η, ζ are three axes such that the z axis (trigonal axis of the crystal) lies in the [111] position of the (ξ,η,ζ) set.

At 4.2°K:

$$\begin{aligned}g&=2.0026\pm0.0005,\\D&=(1719.2\pm1)\times10^{-4}\ \text{cm}^{-1},\\a&=(229.4\pm1)\times10^{-4}\ \text{cm}^{-1},\\a-F&=(341.5\pm1)\times10^{-4}\ \text{cm}^{-1},\\F&=(-112.1)\times10^{-4}\ \text{cm}^{-1}.\end{aligned}$$

The energy levels can be found in the literature. For high external magnetic field ($g\beta H\gg a$) they were obtained by perturbation calculations[15,16] and in the case where $g\beta H$ is of the order of a they were obtained by exact diagonalization of the Hamiltonian.[17] In this latter reference the wave functions are also tabulated.

In corundum the magnetoelastic tensor has only 10

[13] S. Geschwind and J. P. Remeika, Phys. Rev. **122**, 751 (1961).
[14] H. F. Symmons and G. S. Bogle, Proc. Phys. Soc. (London) **79**, 468.
[15] B. Bleaney and R. S. Trenam, Proc. Roy. Soc. (London) **223**, 1 (1954).
[16] B. Bleaney and D. J. E. Ingram, Proc. Phys. Soc. (London) **A205**, 336.
[17] J. Lewiner and P. H. E. Meijer, J. Res. Natl. Bur. Std. **73A**, 241 (1969).

independent coefficients. It can be written as

G_{11}	G_{12}	$-\frac{1}{2}G_{33}$	G_{14}	$-G_{25}$	G_{16}
G_{12}	G_{11}	$-\frac{1}{2}G_{33}$	$-G_{14}$	G_{25}	$-G_{16}$
$-(G_{11}+G_{12})$	$-(G_{11}+G_{12})$	G_{33}	0	0	0
G_{41}	$-G_{41}$	0	G_{44}	G_{45}	G_{52}
$-G_{52}$	G_{52}	0	$-G_{45}$	G_{44}	G_{41}
$-G_{16}$	G_{16}	0	G_{25}	G_{14}	$\frac{1}{2}(G_{11}-G_{12})$.

We have seen that the ion can occupy two nonequivalent magnetic sites. The magnetoelastic terms for these two sites are identical except for the sign of elements[18] G_{52}, G_{25}, G_{16}, and G_{45}.

In all our experiments longitudinal waves were propagated either along the c axis of the crystal or along the a axis. In the first case the only component of the strain that will contribute to $\mathcal{H}_{\text{quad}}$ is ϵ_{zz} and Eq. (3) reduces to

$$\mathcal{H}_{\text{quad}}=\tfrac{3}{2}G_{33}S_z^2\epsilon_{zz}.$$

The only possible transitions then follow the selection rule $\Delta m=0$. In the case of a propagation along the a axis of the crystal the component of the strain is ϵ_{xx} and the Eq. (3) becomes

$$\begin{aligned}\mathcal{H}_{\text{quad}}/\epsilon_{xx}=&\tfrac{1}{2}[\tfrac{1}{2}(G_{11}-G_{12})+iG_{16}]S_+^2\\&+\tfrac{1}{2}[\tfrac{1}{2}(G_{11}-G_{12})-iG_{16}]S_-^2-\tfrac{1}{2}(G_{52}+iG_{41})\\&\times(S_+S_z+S_zS_+)-\tfrac{1}{2}(G_{52}-iG_{41})(S_-S_z+S_zS_-)\\&+\tfrac{1}{2}(G_{11}+G_{12})(S^2{}_-3S_z^2).\end{aligned}\quad(7)$$

Since the Hamiltonian contains terms which can produce $\Delta m=\pm2$, $\Delta m=\pm1$ and $\Delta m=0$, the transitions will now depend on the wave functions in a more complicated way than in the previous case.

III. EXPERIMENTAL PROCEDURE

A. RPA Spectrometer

A standard pulse echo system was used. The block diagram of the system is shown in Fig. 2. The frequency of the ultrasonic wave was 9366 MHz, the pulse width 1 μs. These pulses were used to excite a piezoelectric X-cut quartz transducer bonded to one face of the sample. The ultrasonic pulses were reflected on the opposite face of the sample and produced a series of echoes whose frequency was reduced to an IF frequency. The local oscillator was a 2K25 Klystron whose frequency was locked on the frequency of the magnetron. The pulses were then amplified and detected. The echoes could be either directly observed on an oscilloscope, or fed into a gated amplifier and the amplitude of a selected echo could be recorded as a function of the applied magnetic field.

Two cavities were used. The first one was a cylindrical resonant cavity and the second one was made from a General Radio connector (type GR 900 WN and GR 900 QNJ). This cavity required a higher input power and very fine impedance matchings, but it had the advantage of being nonresonant type and therefore it could be used at any frequency.

The system was in a helium Dewar. An external magnetic field could be swept from 0 to 5000 G.

B. Samples

Different crystals of Fe^{3+}- and Fe^{2+}-doped corundum were used. They were obtained from Linde Air Product Corp. and had been polished by Valpey Crystal Corp. The concentration in weight of Fe^{3+} was 0.05%. The samples were cylindrical rods and the opposite faces were plane within $\frac{1}{10}$ of a wavelength of sodium and parallelism was better than 2 sec of arc.

The transducer was bonded on one face of the rod. The bonding agent was a Dow Corning Silicone reference 510. The bonds were checked at room and nitrogen temperature at the frequency of 1000 MHz.

IV. EXPERIMENTAL RESULTS AND DISCUSSION

A. General Procedure

In a first experiment longitudinal waves were propagated along an a axis of the crystal. The magnetic field was kept perpendicular to this axis and the angle φ between the magnetic field and the a axis was 90° for

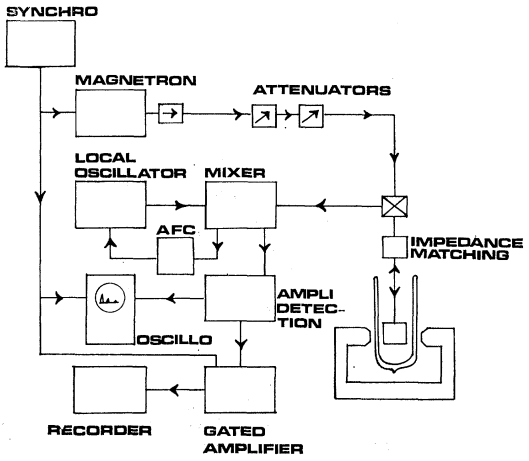

FIG. 2. Block diagram of the APR spectrometer.

[18] T. G. Phillips, R. L. Townsend, and R. L. White, Phys. Rev. 162, 382 (1967).

one site and 30° for the other one. For this orientation the energy levels for the two sites are superimposed.[17] The c axis was kept in a plane perpendicular to the crystal axis and the angle θ between this axis and the magnetic field was varied.

The spectra were taken for values of θ varying from $-100°$ to 110°. The negative values were taken in order to check the symmetry of the observed spectra around the $\theta=0°$ and $\theta=90°$ axes. The results will only be given for values of θ varying from 0° to 90°.

For θ between 0° and 80° many absorption lines were observed for values of the magnetic field between 0 and 5000 Oe. Figure 3 shows a spectrum obtained for $\theta=15°$.

The first problem was to identify the lines and to check that they corresponded to transitions between levels of Fe^{3+} and not of another impurity. The values of the resonant magnetic field for the different observed lines were plotted as a function of the angle θ in Fig. 4. We will characterize the four branches of this figure with the letters a, b, c, and d.

Theoretical $H(\theta)$ curves were constructed for a frequency of 9366 MHz for all possible pairs of energy levels using the tables of Ref. 17. They are plotted in Fig. 5. The six energy levels are labeled from 1 to 6 in order of increasing energies. In Fig. 6 we have superimposed the experimental values of Fig. 4 on the theoretical curves of Fig. 5. It can be immediately observed that branch a coincides with the transition 2–3, branch b with the transition 1–3, and branch d with transition 2-4. However branch c is shifted systematically from the transition 4–5. From this figure we can draw the following two conclusions:

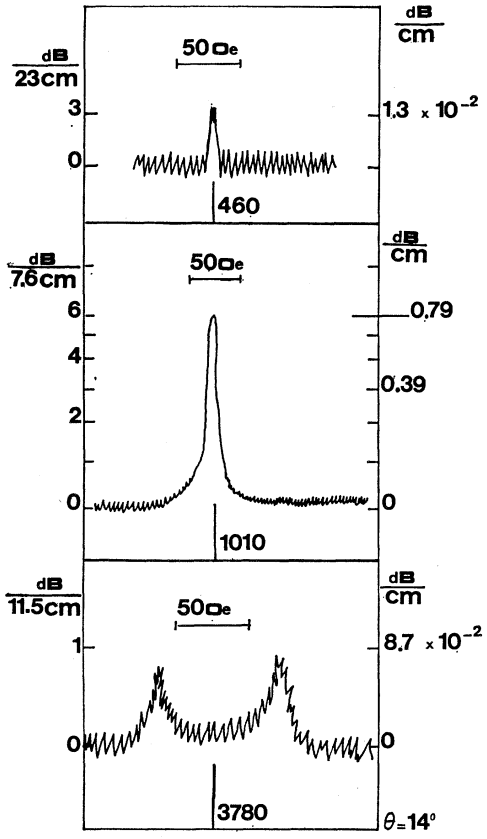

FIG. 3. Ultrasonic absorption spectrum obtained at $\theta=15°$. The top picture shows a line at 460 G. The second is much stronger and has an asymmetric shape with a sharp edge on the high-field side. The bottom picture shows two weak lines around 3780 G of near equal height and similar shape. This pair of lines is the result of two transitions occurring almost symmetrically around a noncrossing point of two levels.

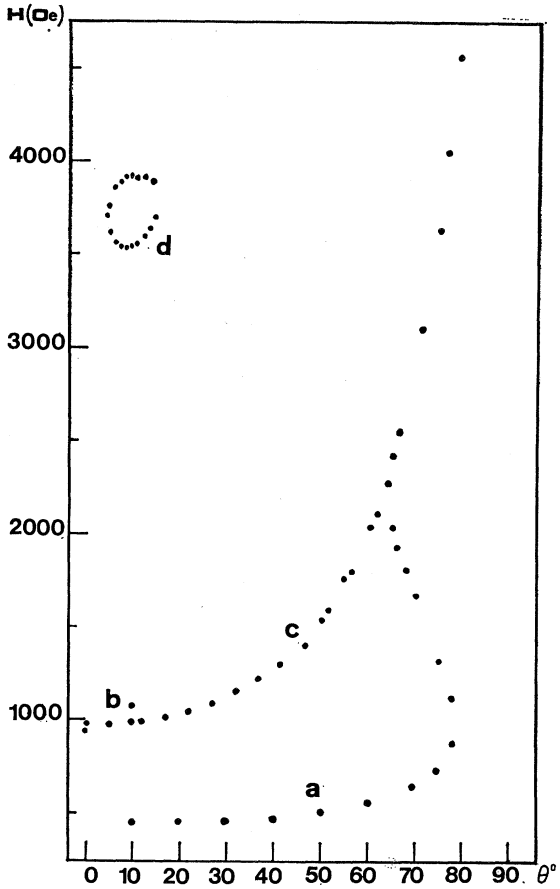

FIG. 4. Experimental curve $H=H(\theta)$, where H represents the value of the magnetic field for the APR lines observed at the angle θ.

(a) Branches a, b, and d are very likely the transitions between different Fe^{3+} levels.

(b) The discrepancy in branch c requires some more investigation. Moreover one has to realize that at least for certain values, the attenuation associated with this branch is almost a hundred times larger than that found in the other branches.

B. Transitions between Fe^{3+} Energy Levels

(1) Let us first consider branch a, which represents the transition 2–3. The dependence of α on θ is given in Fig. 7(a). Using Eq. (5) we can express the absolute

square of the matrix element of the interaction Hamiltonian between the wave functions ψ_2 and ψ_3 as a function of parameters which can either be calculated or measured. We have

$$\frac{|\langle\psi_2|\mathcal{H}_{\text{int}}|\psi_3\rangle|^2}{\epsilon^2}=\frac{4\rho v^3\hbar\alpha}{n\omega g(\nu)}. \tag{8}$$

Here n depends implicitly on the angle θ. Since we do not saturate the transition, it is given by the following

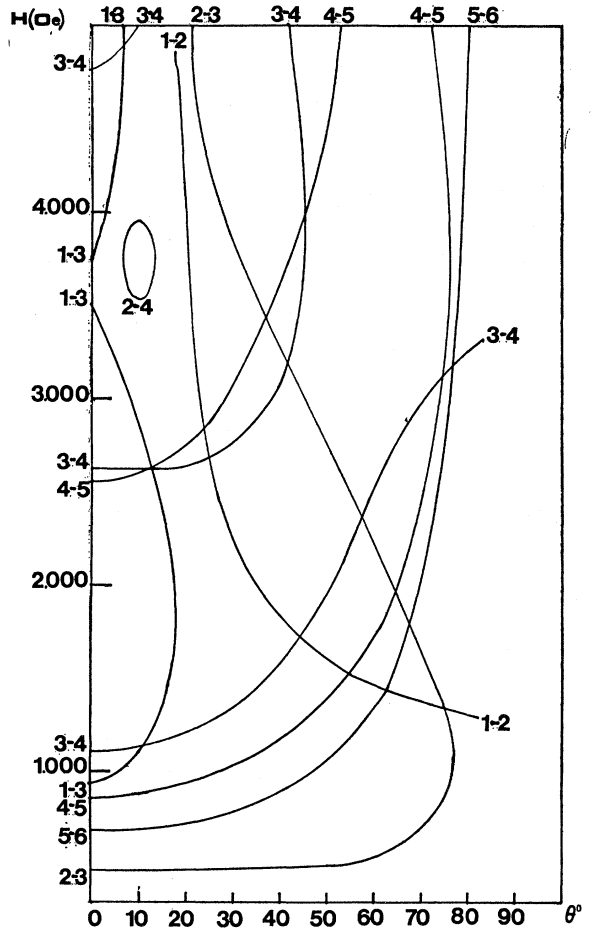

FIG. 5. Theoretical curves $H=H(\theta)$ at the frequency of 9.366 MHz for all the possible pairs of levels.

relation:

$$n=n_2-n_3=N_0(e^{-W_{12}/kT}-e^{-W_{13}/kT})/\sum_{i=1}^{6}e^{-W_{1i}/kT}.$$

In this expression N_0 is the concentration of the Fe^{3+} impurities and $W_{ij}=E_j-E_i$. To calculate $g(\nu)$ it is necessary to approximate the energy difference $F(H)=E_3-E_2$ as a function of H analytically. Since for $\theta=0°$ the energy difference E_3-E_2 can be expressed as a polynomial expansion in H:

$$F(H)=2D+\tfrac{5}{2}(a-F)-2g\beta H+0(H^2). \tag{9}$$

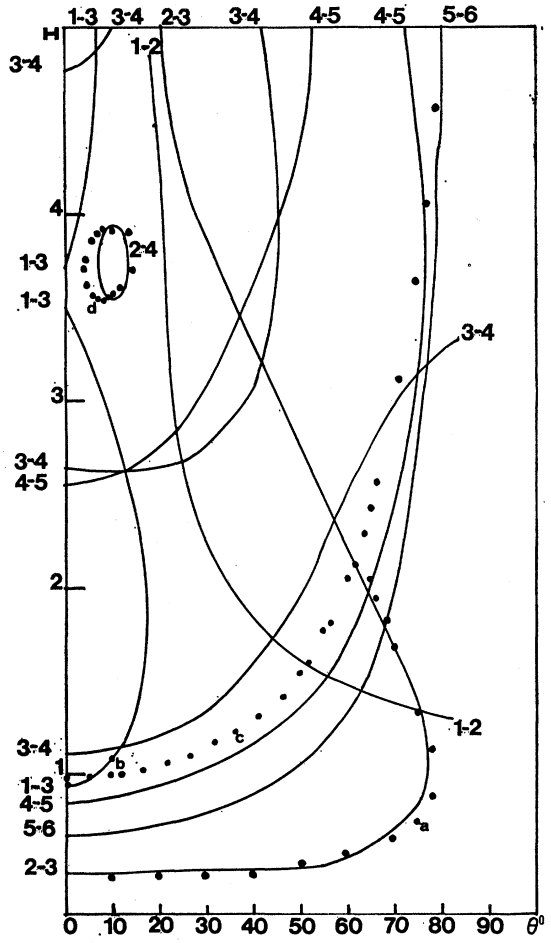

FIG. 6. Superposition of Figs. 4 and 5. Notice that branch a coincides with the transition 2–3, branch b with 1–3, and branch d with 2–4. Branch c is systematically shifted with respect to the transition 4–5.

We can also expand $F(H)$ for an arbitrary direction as a polynomial in H:

$$F(H)=a_0+a_1H+a_2H^2+a_3H^3+a_4H^4+a_5H^5. \tag{10}$$

The coefficients in this expression were obtained by a least square fit. The results are given in Table I. In this table, A is defined as $g(\nu)/f(H)$. From this analysis we have calculated $|\langle\psi_2|\mathcal{H}_{\text{int}}|\psi_3\rangle|^2$ and the results are plotted in Fig. 7(b). Its value for $\theta=0°$ was obtained by extrapolation from this figure. For this particular value of the angle θ, we have the following two wave functions for E_2 and E_3:

$$\psi_2=|\tfrac{1}{2}\rangle+\gamma|-\tfrac{5}{2}\rangle,\quad \psi_3=|-\tfrac{3}{2}\rangle.$$

For the value of the magnetic field H which corresponds to the 2–3 transition at the frequency of 9336 MHz we have $\gamma=0.04$.

We have seen in Sec. II that the interaction Hamiltonian was composed of two terms, the dipolar and

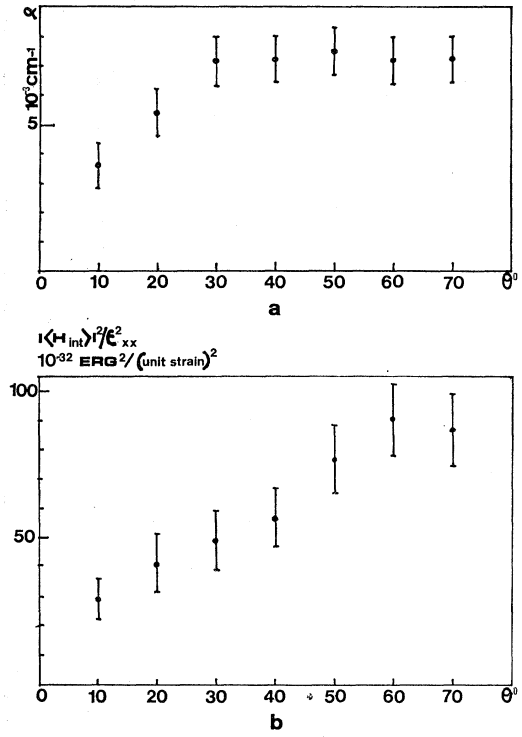

FIG. 7. (a) Dependence of the ultrasonic attenuation α on the angle θ for the 2–3 transition of Fe^{3+}. (b) Dependence of the interaction matrix element on θ for the 2–3 transition of Fe^{3+}.

quadrupolar term. From the wave functions belonging to levels 2 and 3 we find

$$\langle\psi_3|\mathcal{H}_{\rm dip}/\epsilon_{xx}|\psi_2\rangle=-\tfrac{1}{2}\gamma\beta gH(F_{52}+iF_{41})\sqrt{5}\,,$$

and

$$\langle\psi_3|\mathcal{H}_{\rm quad}/\epsilon_{xx}|\psi_2\rangle=3\sqrt{2}[\tfrac{1}{2}(G_{11}-G_{12})-iG_{16}]+2\sqrt{(5)}\gamma(G_{52}+iG_{41})\,.$$

Now we see that the wave functions are such that the quadrupolar term has nonzero matrix elements. Now if we neglect the admixture term in ψ_2 we are left with only one dominant term, which corresponds to a $\Delta m=\pm 2$ transition

$$\langle\psi_3|\mathcal{H}_{\rm int}/\epsilon_{xx}|\psi_2\rangle=3\sqrt{2}[\tfrac{1}{2}(G_{11}-G_{12})-iG_{16}].$$

Let us define

$$G_a{}^2=\tfrac{1}{4}(G_{11}-G_{12})^2+G_{16}{}^2.$$

For this particular angle using Eq. (9) we find that $g(\nu)$ is given by

$$g(\nu)=hf(H)/2g\beta\,,$$

which in turn gives

$$\alpha=9n\pi^2\nu G_a{}^2f(H)/\rho v^3g\beta\,.$$

Finally, we have

$$[\tfrac{1}{4}(G_{11}-G_{12})^2+G_{16}{}^2]^{1/2}=0.42\pm0.11\ \text{cm}^{-1}/\text{unit strain}.$$

In order to interpret the results for $\theta\neq 0$, we need all components of the wave functions. However, many components are small and can be neglected. Keeping only the main components the wave functions can be expressed as

$$\psi_2=(a_1+ib_1)|\tfrac{1}{2}\rangle+(a_2+ib_2)|-\tfrac{1}{2}\rangle\,,$$
$$\psi_3=(a_3+ib_3)|-\tfrac{3}{2}\rangle\,,$$

where the different coefficients are given in Table II for various values of θ. With this approximation we calculate the matrix elements of the quadrupolar interaction Hamiltonian. It is given by

$$|\langle\psi_3|\mathcal{H}|\psi_2\rangle|^2=c_1(X_1{}^2+X_2{}^2)+c_2(X_3{}^2+X_4{}^2)+c_3(X_1X_3+X_2X_4)+c_4(X_1X_4-X_2X_3)\,,\quad(11)$$

where

$$c_1=18(a_3{}^2+b_3{}^2)(a_1{}^2+b_1{}^2)\,,\qquad X_1=\tfrac{1}{2}(G_{11}-G_{12})\,,$$
$$c_2=32(a_3{}^2+b_3{}^2)(a_2{}^2+b_2{}^2)\,,\qquad X_2=G_{16}\,,$$
$$c_3=48(a_3{}^2+b_3{}^2)(a_1a_2+b_1b_2)\,,\qquad X_3=G_{52}\,,$$
$$c_4=48(a_3{}^2+b_3{}^2)(a_1b_2-a_2b_1)\,,\qquad X_4=G_{41}.$$

By calculating c_1, c_2, c_3, c_4 for each value of θ and by comparing the results with Table I, one could hope to obtain the different term in expression (11). Unfortunately the uncertainty in the experiments did not permit us to make a unique determination of the constants.

TABLE I. Coefficients of the polynomial expansion of the function $F(H)/h$, for different values of θ. The constant term is $a_0/h=12.06$. $A=g(\nu)/f(H)$.

θ	a_1/h ($\times10^3$)	a_2/h	a_3/h	a_4/h	a_5/h	A ($\times10^7$)
0	−5.6	$1(10^{-10})$	$-2.2(10^{-13})$	$1.95(10^{-16})$	$-6.06(10^{-20})$	1.8
10	−5.6	$-6.5(10^{-7})$	$1.4(10^{-9})$	$1.2(10^{-12})$	$3.4(10^{-16})$	1.7
20	−5.8	$-5.4(10^{-7})$	$1.8(10^{-9})$	$-1.6(10^{-12})$	$5(10^{-16})$	1.8
30	−6.1	$5(10^{-7})$	$3.2(10^{-10})$	$-3.2(10^{-13})$	$1.7(10^{-16})$	2
40	−6.2	$1.1(10^{-7})$	$-2.9(10^{-10})$	$4.3(10^{-13})$	$-8.6(10^{-17})$	1.96
50	−6.10	$8.5(10^{-7})$	$1.1(10^{-9})$	$-7.5(10^{-13})$	$2.6(10^{-16})$	2.17
60	−5.8	$1.4(10^{-6})$	$4.8(10^{-10})$	$2.1(10^{-13})$	$-1.7(10^{-16})$	2.8
70	−5.6	$2.8(10^{-6})$	$-1.5(10^{-9})$	$1.7(10^{-12})$	$-6(10^{-16})$	5

(2) Now we consider branch b, that is, the transition 1–3. For $\theta=0°$ the wave functions are

$$\psi_1=|-\tfrac{1}{2}\rangle-0.026|\tfrac{5}{2}\rangle,\quad \psi_3=|-\tfrac{3}{2}\rangle.$$

From this we find

$$\langle\psi_1|\mathcal{H}/\epsilon_{xx}|\psi_3\rangle=2\sqrt{(5)}(G_{52}+iG_{41}).$$

Since the transition 1–3 is of the type $\Delta m=1$ in the neighborhood of $\theta=0°$ we have $h\nu=g\beta H$ and $g(\nu)=hf(H)/g\beta$. The value of α can then be written as

$$\alpha=8n\pi\nu G_b^2/g\beta\delta\rho v^3,$$

where

$$G_b^2=G_{52}^2+G_{41}^2,\quad n=N_0(1-e^{-W_{13}/kT})/\sum_{i=1}^{6}e^{-W_{1i}/kT};$$

from these expressions we find

$$[G_{52}^2+G_{41}^2]^{1/2}=2.9\pm0.9\ \text{cm}^{-1}/\text{unit strain}.$$

(3) Branch d corresponds to a 2–4 transition. This transition takes place in a region where the levels 2 and 4 are repelling each other. Consequently the wave functions are strongly mixed. For example for $\theta=15°$ we have

$$\psi_2=-(0.2+i0.2)|\tfrac{1}{2}\rangle+(0.2+i0.4)|-\tfrac{1}{2}\rangle+(-0.1+i0.74)|-\tfrac{3}{2}\rangle+(0.15-i0.26)|-\tfrac{5}{2}\rangle,$$

$$\psi_4=-(0.5+i0.15)|\tfrac{1}{2}\rangle-(0.1+i0.2)|-\tfrac{1}{2}\rangle+(0.2-i0.2)|-\tfrac{3}{2}\rangle+0.8|-\tfrac{5}{2}\rangle.$$

With these wave functions it was impossible to obtain a quantitative result for the matrix elements. It should be noticed however that the typical shape of this branch in Fig. 6 was useful in identifying the transition itself.

C. Analysis of Branch c

As mentioned before this line was systematically shifted from the expected positions of the 4–5 transition of Fe^{3+}. For $\theta=0°$ the wave functions of levels E_4 and E_5 are

$$\psi_4=|\tfrac{3}{2}\rangle,\quad \psi_5=0.999|-\tfrac{5}{2}\rangle+0.04|\tfrac{1}{2}\rangle.$$

Examining these wave functions one is forced to assume a $\Delta m=4$ transition since the observed line is too strong for the $|\frac{3}{2}\rangle\leftrightarrow|\frac{1}{2}\rangle$ transition. Although a $\Delta m=4$ transition is not a priori impossible, it is unlikely that it would produce such a strong line. It was shown experimentally that a small decrease in the ultrasonic frequency produced a decrease in the value of the resonant magnetic field. In the case of a transition between levels E_4 and E_5 of the Fe^{3+} ion one should have observed an increase. This led us to believe that we were observing the transition between two sublevels of a doublet. We have demonstrated[19] that this transition was observed because of the presence of Fe^{2+} ions in the sample, for which we proposed the following spin Hamiltonian:

$$\mathcal{H}=g_{\parallel}\beta H_z S_z+g_{\perp}\beta(H_xS_x+H_yS_y)-D[S_z^2-\tfrac{1}{3}S(S+1)],$$

with an effective spin $S=1$, $g=3.40\pm0.04$, and $D\gg6$ cm^{-1}.

Since for this value of D and for the fields used, $g\beta H\gg D$, we can use a perturbation calculation to derive the energy levels as a function of the angle. This gives up to the fourth order in $g\beta H/D$

$$E_1=-\tfrac{1}{3}D-g_{\parallel}\beta H\cos\theta-\tfrac{1}{2}g_{\perp}^2\beta^2\frac{H^2}{D}\sin^2\theta-\frac{g_{\parallel}g_{\perp}^2\beta^3H^3\sin^2\theta}{8\cos\theta D^2}\times\left[\left(\frac{g_{\perp}}{g_{\parallel}}\right)^2\sin^2\theta-4\cos^2\theta\right]-\tfrac{1}{2}g_{\parallel}^2g_{\perp}^2\beta^4\frac{H^4}{D^3}\sin^2\theta\left[\cos^2\theta-\left(\frac{g_{\perp}}{g_{\parallel}}\right)^2\sin^2\theta\right],$$

$$E_2=-\tfrac{1}{3}D+g_{\parallel}\beta H\cos\theta-\tfrac{1}{2}g_{\perp}^2\beta^2\frac{H^2}{D}\sin^2\theta+\frac{g_{\parallel}g_{\perp}^2\beta^3H^3\sin^2\theta}{8\cos\theta D^2}\times\left[\left(\frac{g_{\perp}}{g_{\parallel}}\right)^2\sin^2\theta-4\cos^2\theta\right]-\tfrac{1}{2}g_{\parallel}^2g_{\perp}^2\beta^4\frac{H^4}{D^3}\sin^2\theta\left[\cos^2\theta-\left(\frac{g_{\perp}}{g_{\parallel}}\right)^2\sin^2\theta\right],$$

$$E_3=\tfrac{2}{3}D+g_{\perp}^2\beta^2\frac{H^2}{D}\sin^2\theta+g_{\parallel}^2g_{\perp}^2\beta^4\frac{H^4}{D^3}\times\sin^2\theta\left[\cos^2\theta-\left(\frac{g_{\perp}}{g_{\parallel}}\right)^2\sin^2\theta\right],$$

and

$$E_2-E_1=2g_{\parallel}\beta H\cos\theta\left[1+g_{\parallel}^2\beta^2\frac{H^2}{D^2}\times\sin^2\theta\frac{(g_{\perp}/g_{\parallel})^2\sin^2\theta-4\cos^2\theta}{8\cos^2\theta}\right].$$

The attenuation of the sound wave was measured for values of θ from 0° to 80° [see Fig. 8(a)]. In order to calculate the matrix elements of the interaction

TABLE II. Tabulated values of the coefficients of the wave functions ψ_2 and ψ_3, for different values of θ.

θ	a_1	b_1	a_2	b_2	a_3	b_3
0	−0.999	0	0	0	1	0
10	−0.97	0.02	−0.2	−0.1	0.999	0
20	−0.9	0.07	−0.4	−0.2	0.998	0
30	−0.86	0.1	−0.5	−0.2	0.99	0
40	−0.81	0.13	−0.51	−0.2	0.99	0
50	−0.8	0.14	−0.6	−0.2	0.99	0
60	−0.8	0.2	−0.6	−0.2	0.98	0
70	−0.7	0.2	−0.6	−0.2	0.96	0.03

[19] J. Lewiner, P. H. E. Meijer, and J. K. Wigmore, Phys. Rev. 185, 546 (1969).

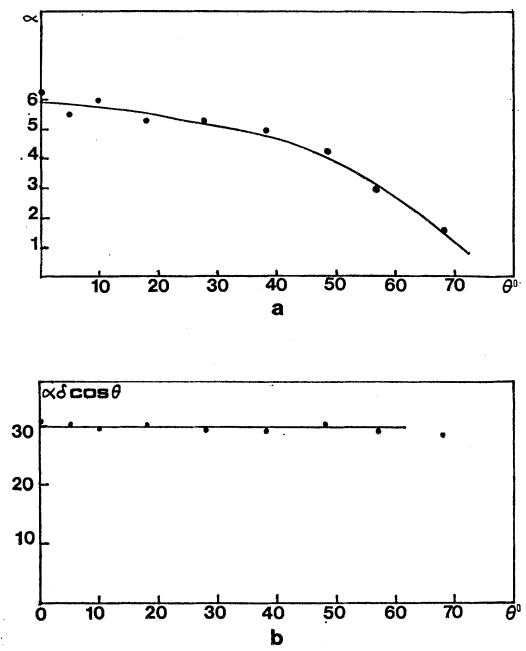

FIG. 8. (a) Sound attenuation of Fe^{2+} as a function of θ. (b) Dependence of $\alpha\delta\cos\theta$ on θ for the Fe^{2+} transition.

Hamiltonian it is necessary to compute the wave functions of levels E_2 and E_3. These wave functions are given in Appendix A. For the sake of simplicity we have assumed an isotropic g factor since $g_{\parallel}$ always equals $g_{\perp}$ within 1% for the iron group ions in Al_2O_3 and since $g_{\perp}$ only appears in terms of second and higher order in $g\beta H/D$. Using these wave functions we obtain

$$|\langle\psi_2|\mathcal{H}_{\text{quad}}/\epsilon_{xx}|\psi_1\rangle|^2=\tfrac{1}{4}(G_{11}-G_{12})^2+G_{16}^2 +[\tfrac{3}{4}(G_{11}^2-G_{12}^2)\sin^2\theta-\tfrac{1}{4}(G_{11}-G_{12})^2\sin^2\theta(1+\tfrac{1}{4}tg^2\theta) -\tfrac{1}{2}G_{52}(G_{11}-G_{12})(3\cos^2\theta-1)-G_{16}^2\sin\theta -G_{41}G_{16}\sin 2\theta](g\beta H/D)^2. \quad (12)$$

Introducing this expression in Eq. (5) it is possible to compare the experimental data with the calculation. The only unknown parameter in this formula is N_0, the concentration of Fe^{2+} in the sample. However we notice that in Eq. (12) the absolute square of the matrix element of the interaction Hamiltonian is independent of θ up to the second order in $g\beta H/D$. To check the validity of this result we expand the other factors of Eq. (5) in this parameter.

TABLE III. Coefficient used in Eq. (11) as a function of θ.

θ	$\cos\theta$	H	α	δ	$\alpha\delta\cos\theta$
0	1	985	6.3	5	31.5
5	0.996	996	5.5	5.5	30.1
10	0.98	1004	6	5	29.4
18	0.95	1038	5.3	6	30.2
28	0.883	1111	5.3	6	28.1
38	0.788	1248	5	7	27.6
49	0.656	1479	4.3	11	31
57	0.545	1848	3	17.5	28.6
68	0.375	2643	1.6	45	27

$$n=\frac{2g\beta H\cos\theta N_0}{kT(2+e^{-D/kT})}\left\{1-\frac{(g\beta H)^2}{2DkT(2+e^{-D/kT})} \times\left[(4+e^{-D/kT})\frac{D\cos^2\theta}{kT}-3\sin^2\theta e^{-D/kT}\right]\right\},$$

$$g(\nu)=hf(H)/2g\beta\cos\theta+\text{second order terms}.$$

Then Eq. (5) can be written as

$$|\langle\psi_1|\mathcal{H}|\psi_2\rangle|^2/\epsilon_{xx}^2=(4\rho v^3kTg\beta/h\nu^2\pi N_0)\alpha\delta\cos\theta. \quad (13)$$

The different factors in this expression are given in Table III. In Fig. 8(b) the experimental values of $\alpha\delta\cos\theta$ are plotted as a function of θ. We notice that this product is independent of the angle θ. This is in good agreement with the theoretical conclusion that the left-hand side of Eq. (13) should also be independent of θ up to second order in $g\beta H/D$. From this we conclude that the spin Hamiltonian and the wave functions which have been used to explain the observed spectra are basically correct.

D. Propagation of Sound Wave along c Axis

In this experiment the sample was placed in such a way that the angle θ between the magnetic field and the c axis could be varied while the angles φ_1, and φ_2 corresponding to the two nonequivalent sites of the lattice were kept equal to 30° and 90°. The angles which characterize the spin system are then exactly the same as those in the first part of the experiment. As mentioned before for this given orientation, the energy levels for the two sites coincide with each other.

For any value of the angle θ no line could be observed by sweeping the magnetic field from 0 to 5000 G. We shall now proceed to show that the absence of any resonance line in this configuration can be explained on the basis of the theory that has been developed so far.

We have seen in Sec. II that the quadrupole interaction Hamiltonian in the case of propagation along the c axis is given by

$$\mathcal{H}_{\text{quad}}/\epsilon_{zz}=\tfrac{3}{2}G_{33}S_z^2.$$

This Hamiltonian gives rise to a $\Delta m=0$ type transition. When expanded on the basis of the free spin eigenfunction, most wave functions will have a dominant component along one basis state. The transition probability between different eigenstates due to this Hamiltonian will therefore be small. The only exception to this rule is found near the noncrossover points in the energy-level scheme, where a strong mixing of the wave functions takes place. Such points, however, are in general associated with energy difference much smaller than the frequency used. Hence we conclude that as a result of the small transition probability, one needs to assume a large value of G in order to observe any

variation of the attenuation. In Fe^{3+} we have seen that the coupling is very weak and the sensitivity of our spectrometer is such that this line should not be observed. On the other hand, we have seen that the coupling for Fe^{2+} is strong, and hence one should consider transitions between the levels of Fe^{2+}. Two possibilities exist. We first calculate the probability of transition between the two sublevels of the lower doublet. Using the wave functions of Appendix A it is found to be

$$|\langle\psi_1|\mathcal{H}_{\text{quad}}/\epsilon_{zz}|\psi_2\rangle|^2=(9/16)G_{33}^2\sin^4\theta(g\beta H/D)^4.$$

As this expression is of *the fourth order* in $g\beta H/D$, this effect should not be observable. The other possibility is that there can be a transition between the singlet and one of the sublevels of the doublet. However because of the very large zero-field splitting it would be necessary to use a very high magnetic field in order to observe the transition at all. Even if such a high magnetic field were reached the effect would hardly be observable because of the strong Boltzmann depopulation factor.

Thus this part of the experiment confirms the hypothesis made for the calculation.

V. CONCLUSIONS

Phillips, Townsend, and White[18] measured the magnetoelastic coupling constants of Fe^{3+} in corundum, using EPR under uniaxial stress. By this method one finds the stress derived magnetoelastic tensor T rather than the strain derived magnetotensor G which is obtained from the APR experiment. In order to compare our experimental results with those of Phillips *et al.*, we first express their results in terms of the G tensor using the following relation (see Appendix B):

$$G=T\cdot C,$$

where we need to know C, the elasticity tensor. Using the tabulated values of the elastic moduli,[20] in this equation we obtain

$$[\tfrac{1}{4}(G_{11}-G_{12})^2+G_{16}^2]^{1/2}=1.55\ \text{cm}^{-1}\ \text{/unit strain},$$

and

$$[G_{52}^2+G_{41}^2]^{1/2}=6\ \text{cm}^{-1}\text{/unit strain}.$$

We observe that although the resulting values are of the same order of magnitude as those obtained by the APR experiment, they lie outside the uncertainty of the errors quoted. This discrepancy could be due to the large uncertainty in the tabulated values of the elastic moduli.

In order to see the effect of a different host material we examine the experimental values which were available for MgO. The symmetry of this lattice is cubic and there are only two independent magnetoelastic coefficients. These coefficients were measured by the APR method by Shiren,[21] who found

$$|G_{11}|=5.0\ \text{cm}^{-1}\text{/unit strain}$$

and

$$|G_{44}|=0.65\ \text{cm}^{-1}\text{/unit strain}.$$

Watkins and Feher[22] measured the same parameters by the EPR under uniaxial stress. They found

$$G_{11}=5.1\ \text{cm}^{-1}\text{/unit strain}$$

and

$$G_{44}=-0.72\ \text{cm}^{-1}\text{/unit strain}.$$

Hence we see that, in spite of the difference in symmetry between the lattices of Al_2O_3 and MgO, their magnetoelastic constants have the same order of magnitude.

Finally we could try to compare our results with the results obtained from first principle calculations. This is a rather difficult problem since the total spin of an S-state ion is coupled to the lattice via second- or higher-order mechanisms. The different theories given in the available literature[23–25] obtain somewhat different results depending on the mechanism chosen to explain this indirect coupling. Among these papers only Leushin[25] makes some explicit calculation on the Fe^{3+} ion.

The analysis of the Fe^{2+} transition, going beyond the observations made in our previous publication,[19] has lead to the following results. The energy levels and the wave functions were calculated and using these it was possible to calculate the theoretical dependence of the ultrasonic attenuation on the angle θ. The good agreement between the calculated and observed values confirmed the general hypotheses made for the spin Hamiltonian and the wave functions. Moreover, we did not observe any transition while sound was propagated along the c axis, which confirms the theoretical prediction that the lines should be either of the fourth order and hence hardly observable or should be such that the Boltzmann depopulation factor would make it unobservable.

If we compare our numerical data with those obtained by Low and Weger[26] for Fe^{2+} in MgO, we notice that they could describe their results by the following spin Hamiltonian:

$$\mathcal{H}=g\beta H\cdot S,\quad S=1$$

where $g=3.428$. This implies that the ground level of MgO is a triplet. However in our case we are not dealing with a cubic field, and hence this triplet is split into a doublet and a singlet. The doublet lies lower than the singlet and the splitting is larger than 6 cm^{-1}. Our

[20] Landolt-Börnstein, *Numerical Data and Functional Relationships in Science and Technology. Group III: Crystal and Solid State Physics* (Springer-Verlag, Berlin, 1966), Vol. 1.

[21] N. S. Shiren, Bull. Am. Phys. Soc. **7**, 29 (1962).

[22] G. D. Watkins and E. R. Feher, Bull. Am. Phys. Soc. **7**, 29 (1962).

[23] M. Blume and R. Orbach, Phys. Rev. **127**, 1587 (1962).

[24] J. Kondo, Progr. Theoret. Phys (Kyoto) **28**, 1026 (1962).

[25] A. M. Leushin, Fiz. Tverd. Tela **5**, 605 (1963) [English transl.: Soviet Phys.—Solid State **5**, 440 (1963)].

[26] W. Low and M. Weger, Phys. Rev. **118**, 1130 (1960).

g factor is the same as those obtained by them. Stevens and Walsh[27] found that the ground state of the Fe^{2+} ion in corundum is indeed of this configuration with a splitting factor of 100 cm^{-1}, which is not in contradiction with our result.

As before, in order to see the effect of a different host material, we look at the values which were available for MgO. Shiren[21] obtained by APR the following values:

$$|G_{11}| = 650 \text{ cm}^{-1}/\text{unit strain}$$

and

$$|G_{44}| = 380 \text{ cm}^{-1}/\text{unit strain}.$$

The same parameters were measured by EPR under uniaxial stress by Watkins and Feher[23] and they obtained

$$G_{11} = 800 \text{ cm}^{-1}/\text{unit strain}$$

and

$$G_{44} = 540 \text{ cm}^{-1}/\text{unit strain}.$$

We found that the magnetoelastic constants are larger than 15 cm^{-1} in corundum. It was not possible to give the exact value of this constant, because of the unknown concentration of Fe^{2+} in the sample. However it seems unlikely that the magnetoelastic constants would be as large as those in MgO, since this would require us to assume an unusually low concentration of Fe^{2+} ions in the sample. In their theoretical calculation Stevens and Walsh concluded that the coupling should be much smaller than in MgO. This is consistent with our arguments.

They also conclude that the ion is weakly coupled to the lattice. This however, does not seem to be the case.

In a recent publication[28] Kopvillem *et al.* measured the acoustical relaxation of Fe^{3+} in Al_2O_3. They were not able to observe the resonance absorption of sound because of the small spin lattice coupling. By a relaxation (or nonresonance) acoustic paramagnetic absorption experiment they obtained the order of magnitude of the spin-phonon interaction. Their orders of magnitude are consistent with our results.

ACKNOWLEDGMENTS

The authors would like to acknowledge the assistance provided by J. Lally and Dr. R. Meister, and to thank Dr. S. M. Bose and Dr. J. Korringa for their critical reading of the manuscript.

[27] K. W. H. Stevens and D. Walsh, J. Phys. C. **2**, 1 (1968); **2**, 1554 (1968).

[28] U. K. H. Kopvillem and B. P. Smolyakov, Fiz. Tverd. Tela **11**, 320 (1969) [English transl.: Soviet Phys.—Solid State **11**, 256 (1969)].

APPENDIX A: WAVE FUNCTIONS OF THREE LOWER LEVELS OF Fe^{2+} IN Al_2O_3

We define the wave functions as

$$\psi_1 = x_1|-1\rangle + y_1|+1\rangle + z_1|0\rangle,$$
$$\psi_2 = x_2|-1\rangle + y_2|+1\rangle + z_2|0\rangle,$$
$$\psi_2 = x_3|-1\rangle + y_3|+1\rangle + z_3|0\rangle,$$

$$x_1 = -1 + \tfrac{1}{4}(\sin^2\theta)(1+\tfrac{1}{8}tg^2\theta)(g\beta H/D)^2,$$
$$y_1 = -(\sin^2\theta/4\cos\theta)(g\beta H/D) + \tfrac{1}{4}(\sin^2\theta)(g\beta H/D)^2,$$
$$z_1 = (\sin\theta/\sqrt{2})(g\beta H/D) - (tg\theta/4\sqrt{2})(5\cos^2\theta - 1)(g\beta H/D)^2,$$
$$x_2 = (\sin^2\theta/4\cos\theta)(g\beta H/D) + \tfrac{1}{4}(\sin^2\theta)(g\beta H/D)^2,$$
$$y_2 = -1 + \tfrac{1}{4}(\sin^2\theta)(1+\tfrac{1}{8}tg^2\theta)(g\beta H/D)^2,$$
$$z_2 = (\sin\theta/\sqrt{2})(g\beta H/D) + (tg\theta/4\sqrt{2}) \times (5\cos^2\theta - 1)(g\beta H/D)^2,$$
$$x_3 = (\sin\theta/\sqrt{2})(g\beta H/D) - (\sin\theta\cos\theta/\sqrt{2})(g\beta H/D)^2,$$
$$y_3 = (\sin\theta/\sqrt{2})(g\beta H/D) + (\sin\theta\cos\theta/\sqrt{2})(g\beta H/D)^2,$$
$$z_3 = 1 - \tfrac{1}{2}(\sin^2\theta)(g\beta H/D)^2.$$

APPENDIX B: TRANSFORMATION OF MAGNETOELASTIC TENSOR

In this appendix we transform the stress derived magnetoelastic tensor into the strain derived magnetoelastic tensor. This is done by using the elastic moduli. The magnetoelastic tensors can be transformed in the following manner:

$$d_{ij} = \sum_{kl} T_{ijkl}\sigma_{kl},$$
$$\sigma_{kl} = \sum_{mn} C_{kl\,mn}\epsilon_{mn},$$
$$d_{ij} = \sum_{kl} T_{ijkl} \sum_{mn} C_{kl\,mn}\epsilon_{mn} = \sum_{kl}\sum_{mn} T_{ij\,kl}C_{kl\,mn}\epsilon_{mn} = \sum_{mn} G_{ij\,mn}\epsilon_{mn}.$$

If we take the symmetry of corundum into consideration, there are only six independent elastic constants. Using Voigt's notation, we have

$$C_{11} = 49.4, \quad C_{12} = 15.8,$$
$$C_{33} = 49.6, \quad C_{13} = 11.4,$$
$$C_{44} = 14.5, \quad C_{14} = -2.3,$$

in units of 10^{11} dyn/cm^2.